Non-invasive and wearable thermometer for continuous monitoring of core body temperature under various convective conditions

D. Matsunaga, Y. Tanaka, M. Seyama, and K. Nagashima

***Abstract*— We describe the design of a thermometer that can be worn during everyday activities for monitoring core body temperature (CBT) at the skin surface. This sensor estimates the CBT by measuring the heat flux from the body core based on a thermal conductive model. The heat flux is usually affected by the ambient convective conditions (e.g. air conditioner or posture), which in turn affects the model's accuracy. Thus, we analytically investigated heat conduction and designed a sensor interface that would be robust to convection changes. We performed an *in vitro* experiment and a preliminary *in vivo* experiment. The accuracy of CBT in an *in vitro* experiments was 0.1°C for convective values ranging from 0 to 1.2 m/s. The wearable thermometer has high potential as non-invasive CBT monitor.**

I. Introduction

The core body temperature (CBT) is closely related to the activity state of the brain and organs [1]. Hence, it plays an important role in medicine and healthcare, by giving information on patient's condition under anesthesia, during surgery and in intensive care, etc. In addition, we are interested in using the relationship between circadian rhythm and CBT, as a means of advanced health management for, e.g. sleep quality improvement [2]. The CBT moves with an amplitude of about 1°C during a day and is synchronized with the circadian rhythm [3]. Monitoring of circadian rhythm requires an accurate CBT measurement (e.g. ± 0.1°C). Current CBT measurement techniques require a sensor interface to be inserted into the body (e.g. rectum, esophagus, or ear membrane) [4, 5], which is highly invasive and stressful. Hence, ingestible or skin-attachable sensors have been proposed and investigated as alternatives. While an ingestible sensor is not affected by the ambient environment [6], it is affected by meals and the activity of the digestive organs. It is discharged from the body within 24 hours. On the other hand, a skin-attachable sensor provides continuous measurements without causing any stress on the individual [7]. However, it is affected by ambient disturbances, which restricts its use cases. Some methods use a heater to reduce ambient effects. However, this enlarges the system and consumes energy [8]. In this study, we improved the thermal equivalent circuit model and designed a thermometer for CBT monitoring by undertaking analytical and experimental investigations considering the effect of convective conditions. Then, we devised a skin-attachable sensor that lessens effects of ambient disturbances. We used this sensor to perform CBT measurement in an *in vitro* experiment and in a preliminary *in vivo* experiment and found that its measurement error is within ± 0.1°C.

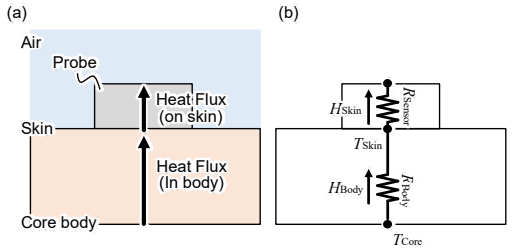

Figure 1. Existing CBT estimation model and thermal equivalent circuit model for a skin-attachable sensor.

II. Non-invasive CBT Measurement

The CBT estimation model and a thermal equivalent circuit for a skin-attachable sensor were first developed by R.H. Fox et al. [8]. As shown in Fig. 1, they model heat transfer from the body to the ambient by using Eq. (1). The CBT, T_{Core}, is estimated from the skin surface temperature, T_{Skin}, the thermal resistance of the body, R_{Body}, and the measured heat flux, H_{Skin}.

$$T_{\mathrm{Core}} = T_{\mathrm{Skin}} + R_{\mathrm{Body}} \cdot H_{\mathrm{Skin}} \tag{1}$$

This model requires R_{Body}, which is generally difficult to obtain, for estimation of T_{Body}. Approaching this issue, dual heat flux method (DHFM) [7] has proposed, which R_{Body} is canceled out by using two heat flux paths. T_{Core} is given by

$$T_{\mathrm{Core}} = \frac{KT_{\mathrm{Skin1}}H_{\mathrm{Skin2}} - T_{\mathrm{Skin2}}H_{\mathrm{Skin1}}}{KH_{\mathrm{Skin2}} - H_{\mathrm{Skin1}}} \tag{2}$$

K is a constant coefficient obtained by using the initial T_{Core} (e.g. tympanic temperature sensor.) at the beginning of measurement [9]. The DHFM assume that there is no heat flows out side of sensor. However, K is a function of the thickness of the body or R_{Body} [9]. R_{Body} can not be canceled out, once the R_{Body} changes. As shown in Fig. 2 (a), it may be caused by heat flux to leak directly into the ambient instead of that is considered by DHFM. It due to distortions in the temperature distribution in the body caused by the thermal resistance of the sensor probe, R_{Sensor}. Hence, as shown in Fig. 2(b), we improve the thermal equivalent circuit model that takes this leakage flux into account as lumped parameter model. T_{Air}, R_{Air}, R_{Sensor}, and H_{Body} denote the ambient temperature, thermal resistance to ambient air, thermal

D. Matsunaga, Y. Tanaka, and M. Seyama are with NTT Device Technology Labs, NTT Bio-Medical Informatics Research Center, NTT Corporation, Atsugi, Japan (phone: +81-46-240-2819; e-mail: {daichi.matsunaga.ye, yujiro.tanaka.cw, michiko.seyama.bm}@hco.ntt.co.jp).

K. Nagashima is with Body Temperature and Fluid Laboratory (Laboratory of Integrative Physiology), Faculty of Human Sciences, Waseda University, Tokorozawa, Japan (e-mail: k-nagashima@waseda.jp).

978-1-7281-1990-8/20/$31.00 ©2020 IEEE

resistance of the probe, and heat flux in the body, respectively. H_{Leak} and R_{Leak} denote leaked heat flux and the thermal resistance of the H_{Leak} path. In this circuit, T_{Core} is given by

$$\begin{aligned} T_{\mathrm{Core}} &= T_{\mathrm{Skin}} + R_{\mathrm{Body}} \cdot H_{\mathrm{Body}} \\ &= T_{\mathrm{Skin}} + R_{\mathrm{Body}} \cdot \alpha H_{\mathrm{Skin}} \end{aligned} \tag{3}$$

$$\alpha = (H_{\mathrm{Skin}} + H_{\mathrm{Leak}})/H_{\mathrm{Skin}} \tag{4}$$

$$R_{\mathrm{Body}} \cdot \alpha = (T_{\mathrm{Core}}(0) - T_{\mathrm{Skin}}(0))/H_{\mathrm{Skin}}(0) \tag{5}$$

The α is a coefficient for calibration, which reflects the ratio of H_{Skin} and H_{Leak} in Eq. (4). It can be calibrated by the initial CBT, $T_{\mathrm{Core}}(0)$, obtained by another method together with R_{Body} in Eq. (5), as in the ordinary methods [9]. H_{Skin} and H_{Leak} are given by an expression derived from the first and second laws of Kirchhoff. Consequently, α can be expressed as a function of thermal resistance by using Eq. (4),

$$\alpha = 1 + \frac{R_{\mathrm{Body}} R_{\mathrm{Sensor}}}{R_{\mathrm{Air}}(R_{\mathrm{Leak}} + 2R_{\mathrm{Body}}) + R_{\mathrm{Leak}} R_{\mathrm{Body}}} \tag{6}$$

In Eq. (6), α does not depend on T_{Core} or T_{Air}. If only these temperatures changes occur, it does not affect the ratio of H_{Skin} and H_{Leak}, so α does not change and no estimation error occurs. R_{Body} and R_{Leak} mainly depend on the thickness of the human body at the measurement point, so they can be considered to be constants. In addition, R_{Sensor} is also constant. However, considering the limitations in reducing the size and thickness of the sensors that measure H_{Skin} and T_{Skin}, the design of a sensor with negligibly small R_{Sensor} is difficult. Hence, α still depends on R_{Air} which is affected by convection changes (e.g. wind), and which in turn causes H_{Skin} and H_{Leak} to change at different rates due to the presence of R_{Sensor}. In this case, α changes, and estimation errors occur.

The thermal equivalent circuit in Fig. 2 (d) bridges R_{Air} over R_{Sensor} and R_{Air} on the skin. In this bridge circuit, T_{Core} is the same as Eq. (3). H_{Skin} and H_{Leak} are also given by the first and second laws of Kirchhoff. Hence, from Eq. (4), α can be expressed as a function of thermal resistance.

$$\alpha = 1 + \frac{R_{\mathrm{Sensor}}}{R_{\mathrm{Leak}}} \tag{7}$$

In Eq. (7), α does not depend on R_{Air}. In other words, α does not change even when R_{Air} changes due to convection, and consequently, estimation errors do not occur. This concept can be realized by wrapping the probe with a highly thermally conductive material, as shown in Fig. 2(c). The leaked heat flux is made to pass through the thermally conductive material. Hence, we call this structure a heat flux path control structure.

III. Experiment & Result

A. Computational simulation

We verified our heat flux path control structure by computational simulation. A heat conduction analysis was performed in the steady state using a finite element method (FEM). The FEM simulation was performed using COMSOL

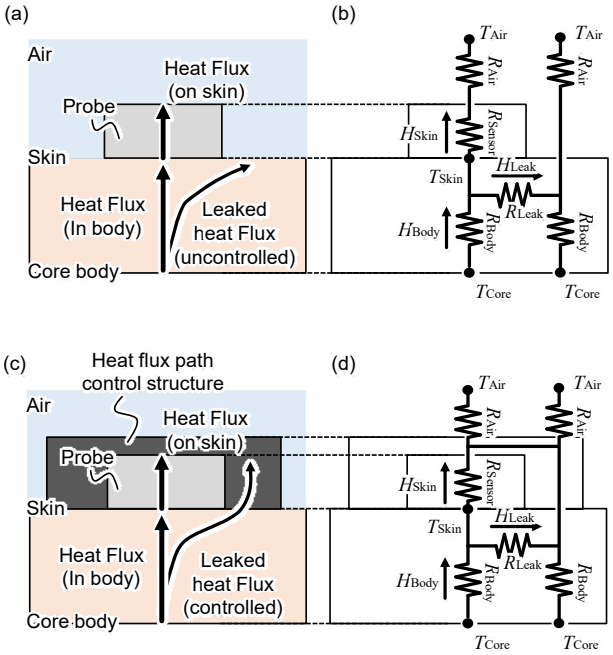

Figure 2. CBT estimating model and thermal equivalent circuit model taking leaked heat flux into consideration. (a) and (b) are those of ordinary techniques. (c) and (d) are those of the proposed technique.

Multiphysics®. The boundary conditions for the heat conduction analysis were as follows.

$$\begin{aligned} &-\lambda\left(\frac{\partial T}{\partial x} + \frac{\partial T}{\partial y} + \frac{\partial T}{\partial z}\right) \\ &= h(T_{\mathrm{Air}} - T) + \varepsilon\sigma\left({T_{\mathrm{Air}}}^4 - T^4\right) \end{aligned} \tag{8}$$

λ, h, ε, and σ respectively denote the thermal conductivity of the body tissue, the heat transfer coefficient of the convection of the ambient air, the emissivity, and the Stefan–Boltzmann constant. R_{Body} is determined from the distance from the skin surface to the CBT area in the body (called the thickness of the body). The probe was attached to the forehead as in other studies [9, 10], and the thickness of the body was 10 mm. The thermal conductivity and the emissivity of the body were typical values for skin and bone, 0.37 W/m·K and 0.96. The heat flux control structure was made of aluminum, which has a thermal conductivity of 236 W/m·K and emissivity of 0.04. The probe was 10 mm thick. The thermal conductivity of the probe was 0.02 W/m·K, assuming the use of phenol foam, which does not expand or deform with temperature and has stable contact resistance. Figures 3 (a) and (b) show examples of the simulated temperature distribution. Unlike in Fig. 3 (a) where the heat flux leaks directly into the ambient air, the heat flux leakage passes through the proposed structure in Fig. 3 (b). This result indicated that the probe should be able to control heat flux leakage.

If the heat flux path control structure is infinitely large, all leaked heat flux can be controlled. However, the sensor is to be attached to a human body so it should not be bulky. CBT estimation errors may occur even a slight leaked heat flux cannot be controlled. Therefore, we optimized the size of the structure by computational simulation. As shown in Fig. 3 (b), the size of the probe was set to Φ 28 mm to accommodate a

20-mm-square heat flux sensor. T_{Core} was set to 37ºC. The ambient air temperature T_{Air} was set to 24 or 28ºC. The temperature differences between T_{Core} and T_{Air} were thus 9 and 13ºC. The size of the structure was varied from 1 to 10 mm in 1 mm steps. Although it is difficult to determine the heat transfer coefficient from the convection state of the ambient air, representative values for natural and forced convection are 5 to 20 and 20 or more W/m^2·K. Figure 3 (c) shows the simulated relationship between the proposed structure and the estimation error when h was varied from 10 W/m^2·K (natural convection) to 30 W/m^2·K (forced convection). The estimation error was defined as the difference between the CBT estimated by Eq. (3) and the reference CBT. When the size of the structure is 0 mm, the probe is the same as the ordinary probe. The proposed probe with a total size of Φ 38 mm can reduce the estimation error by 0.3ºC in comparison with the conventional probe. Here $R_{Body}\alpha$ is 0.059 K/W. In addition, as the proposed structure becomes smaller, more of the leaked heat flux cannot be controlled and the estimation error tends to increase. However, the structure is larger than 5 mm, the effect of the uncontrolled leaked heat flux is small.

B. *In vitro*

On the basis of the results of the simulation, we fabricated a Φ 38 mm probe that contained a 20-mm-square heat flux sensor, a thermistor, and a 5-mm thick heat flux control structure. Figure 4 (a) shows schematic diagram of the *in vitro* experimental system and an illustration of the sensor probe and the heat flux control structure. The heat flux sensor (Denso, special order) consisted of a thin film with a thickness of 0.25 mm and it output a heat flux measurement as a voltage. The output data resolution after analog to digital conversion was about 0.01 W/m·K. The thermistor (TE Connectivity, TSYS01) had a built-in AD converter, and the output data resolution was 0.01°C. We created the probe by stacking these two sensors. The output from the probe was transmitted from the logger to a PC wirelessly via Bluetooth. The experiment was conducted in a thermostat chamber. T_{Air} was set at 28°C, i.e. room temperature. The temperature of the hot plate was used as T_{Core}. The output data resolution of the reference T_{Core} was 0.01°C. T_{Core} was set to 37°C or 41°C in order to simulate a case where the temperature difference between T_{Core} and T_{Air} was 13°C, e.g. T_{Core} = 37°C and T_{Air} = 24°C. The body phantom was made of ethylene propylene rubber (EPDM), which has thermal properties close to those of body tissue. The thermal conductivity of EPDM was 0.36 W/m·K. The thickness of the phantom was 10 mm. The outside air was convected by a pulse width modulation fan installed in the thermostat chamber. The wind velocity was controlled by the fan controller. The wind velocity was measured with a hot-wire anemometer (Satotech, KAM-003-J1) installed near the probe. The data output resolution was 0.01 m/s. Figure 4 (b) shows the experimental relationship between wind velocity and estimation error, when the wind velocity was varied from 0 to 1.2 m/s. The estimation error is defined as the difference between the CBT estimated by Eq. (2) and the reference CBT. Although the estimation error tends to increase slightly as the wind velocity increases and the convection of the ambient air increases, it stays within ±0.1°C at any wind velocity. Here $R_{Body}\alpha$ is 0.051 K/W. The *in vitro* experiment thus showed that CBT can be estimated to within 0.1°C in a state in which convection changes.

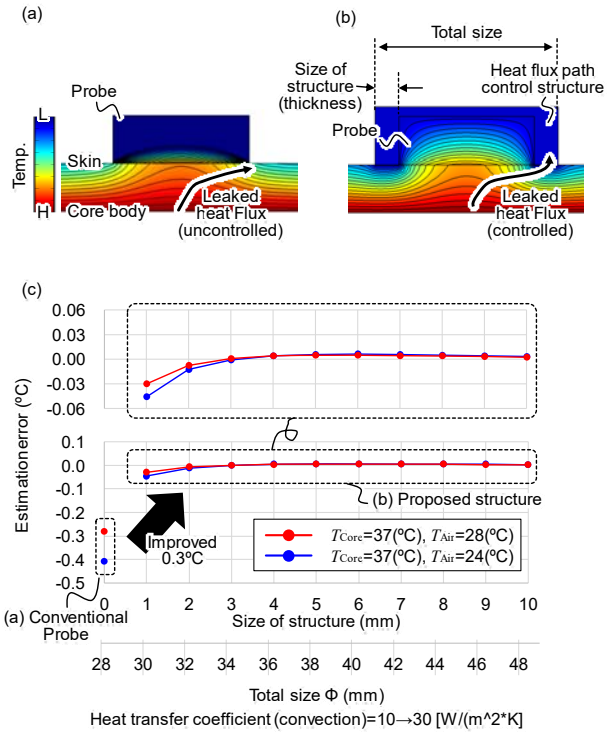

Figure 3. Optimization of the design of the proposed heat flux path control structure. (a) Example of temperature distribution in ordinary probe. (b) Example of temperature distribution in proposed probe. (c) Simulated relationship between structure size and estimation error.

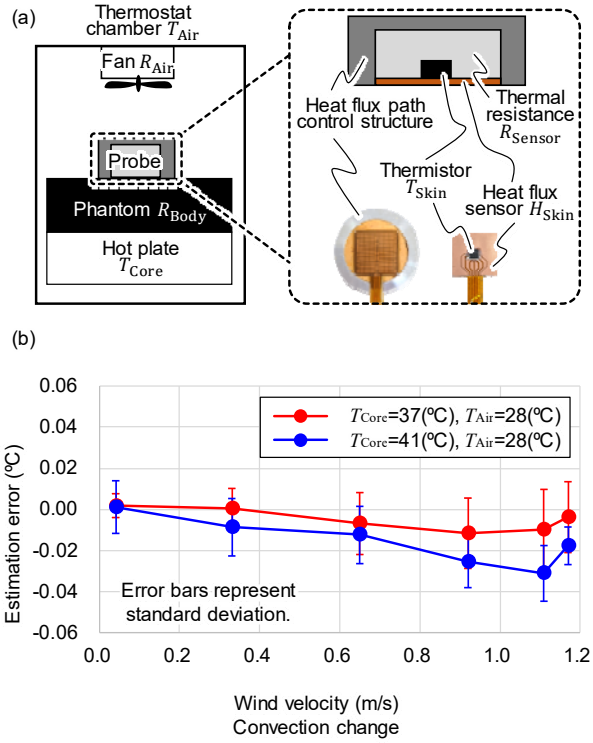

Figure 4. *In-vitro* experiment. (a) Schematic diagram of experimental system and magnified illustration of sensor probe and proposed structure. (b) Experimental relationship between wind velocity (ambient convection) and estimation error. The estimation error is within ±0.1ºC even in an environment in which convection changes.

C. *In vivo*

We performed a preliminary *in vivo* experiment with the aim of developing a wearable CBT sensor for practical use. 3 healthy subjects (2 males, 1 female, 22.7 ± 2.7 years old) participated. The experiment procedures were approved by the ethical committee of Waseda University and conducted according Declaration of Helsinki. Figure 5 (a) shows a schematic diagram. The experiment was performed in an environmental chamber. T_{Air} was set to 28°C, which is in the thermoneutral zone where heat diffusion by perspiration does not occur. Consequently, that the estimation error can be evaluated from only convection of the ambient air. Relative humidity was set at 50%. The reference T_{Core} was measured with an infrared tympanic thermometer (Nipro, CE Thermo). The experiment was performed while suppressing the fluctuation of the referenced value due to the convection change. The same probe as used in the *in vitro* experiment was attached to the forehead as in other studies [9, 10]. The ambient air was convected by a fan installed in the environmental chamber, and the wind velocity was adjusted to about 1 m/s by using the value measured with a hot-wire anemometer installed near the head. During the experiment, the subject remained seated. The subject could drink water freely. Figure 5 (b) shows the example time-series of experimental wind velocity and estimated CBT. After mounting the sensor and the value measured by the reference sensor reached a steady state (0 min.), we varied the convection for 60 minutes. Although, an error during the unsteady state was observed immediately after the convection change caused by heat capacity of a body, the estimation error in the steady state was 0.1°C or less. The experimental results are summarized in Table 1. These results indicate that the probe can measure accurately even when the convection changes.

IV. Conclusion

We developed a wearable device that measures core body temperature from the skin surface in environments where convection changes. This technique is based on indirect estimation of the core body temperature using heat flux. To reduce estimation errors caused by changes in convective conditions, we created a new two-dimensional thermal equivalent circuit model and devised a probe with a heat flux control structure. We optimized the probe size in a computational simulation, and performed an *in vitro* experiment and a preliminary *in vivo* experiment. The estimation error caused by convective changes was successfully reduced within 0.1°C. In future work, we will miniaturize the probe size and evaluate its accuracy in different environments such as during exercise.

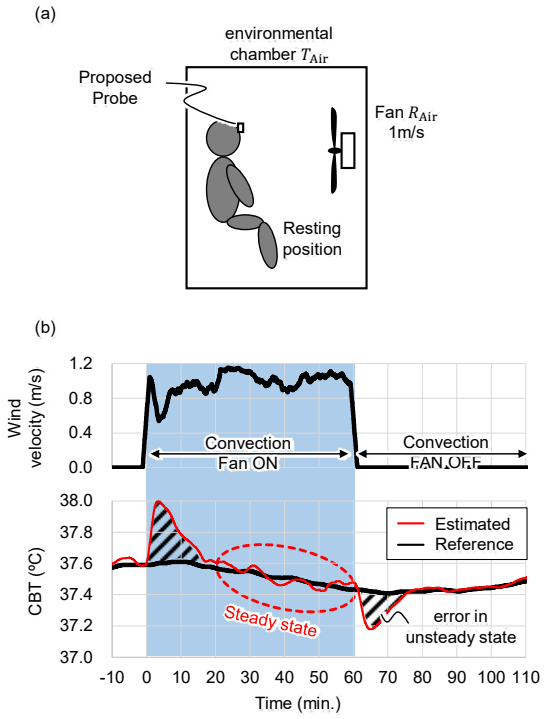

Figure 5. *In vivo* experiment. (a) Schematic diagram of experimental system. (b) Experimentally measured wind velocity and estimated CBT. Black and red lines respectively denote reference CBT and estimated CBT. An error occurs immediately after the ambient air convection changes, but estimated CBT returns to a stationary state in about 20 minutes.

Table 1. The experimental results

Subject	Average error (AE) (°C)	Standard deviation (SD) (°C)	$R_{\mathrm{body}}\alpha$ (K/W)
#1	0.01	0.03	0.033
#2	-0.00	0.03	0.028
#3	0.02	0.02	0.027

References

[1] A.A. Romanovsky, "Thermoregulation: some concepts have changed. Functional architecture of the thermoregulatory system," *Am J Physiol Regulatory Integrative Comp Physiol*, 292, R37–R46, 2007.

[2] N. Obradovich, R. Migliorini, S.C. Mednick, and J.H. Fowler, "Nighttime temperature and human sleep loss in a changing climate," *Sci. Adv.*, vol. 3, no. 5, e1601555, 2017.

[3] S. Mendt, M.A. Maggioni, M. Nordine, M. Steinach, O. Opatz, D. Belavý, D. Felsenberg, J. Koch, P. Shang, H.C. Gunga, and A. Stahn, "Circadian rhythms in bed rest: Monitoring core body temperature via heat-flux approach is superior to skin surface temperature," *Chronobiol. Int.*, vol. 34, pp. 666–676, 2017.

[4] S.M. Lee, W.J. Williams, and S.M. Schneider, "Core temperature measurement during supine exercise: Esophageal, rectal, and intestinal temperatures," Aviat Space Environ Med., vol. 71, pp. 939–945, 2000.

[5] S.K. Chaung, "Tympanic Temperature Measurement: Comparison among the Insertion Methods," *International Information Institute*, vol. 19, pp. 4589–4593, 2016.

[6] S. Yoshida, H. Miyaguchi, and T. Nakamura, "Development of basic system of ingestible core body thermometer with small size and low energy consumption powered by gastric acid battery," *Proc. IEEE Sen.*, pp. 1–3, 2017.

[7] K. Kitamura, X. Zhu, W. Chen, and T. Nemoto, "Development of a new method for the noninvasive measurement of deep body temperature without a heater," *Med. Eng. Phys.*, vol. 32, pp. 1–6, 2010.

[8] R.H. Fox, A.J. Solman, R. Issacs, A.J. Fry, and I.C. Macdonald, "A New Method for Monitoring Deep Body Temperature from the Skin Surface," *Clin. Sci.*, vol. 44, pp. 81–86, 1973.

[9] J. Feng, C. Zhou, C. He, Y. Li, and X. Ye, "Development of an improved wearable device for core body temperature monitoring based on the dual heat flux principle," *Med. Eng. Phys.*, vol. 38, no. 4, pp. 652–668, April 2017.

[10] M. Huang, T. Tamura, W. Chen, and S. Kanaya, "Evaluation of structural and thermophysical effects on the measurement accuracy of deep body thermometers based on dual-heat-flux method," *J. Therm. Biol.*, vol. 47, pp. 26–31, Jan. 2015.